Herpes simplex virus induces extensive modification and dynamic relocalisation of the nuclear mitotic apparatus (NuMA) protein in interphase cells

Yohei Yamauchi, Kazuya Kiriyama, Hiroshi Kimura and Yukihiro Nishiyama*

Department of Virology, Graduate School of Medicine, Nagoya University, Tsurumai-cho 65, Showa-ku, Nagoya 466-8550, Japan
*Author for correspondence (e-mail: ynishiya@med.nagoya-u.ac.jp)

Accepted 8 April 2008
Journal of Cell Science 121, 2087-2096 Published by The Company of Biologists 2008
doi:10.1242/jcs.031450

Summary

The nuclear mitotic apparatus (NuMA) protein is a component of the nuclear matrix in interphase cells and an essential protein for the formation of mitotic spindle poles. We used herpes simplex virus (HSV), an enveloped DNA virus that replicates in the nucleus, to study the intra-nuclear dynamics of NuMA in infected cells. This study shows that NuMA is extensively modified following HSV infection, including phosphorylation of an unidentified site(s), and that it depends to an extent on viral DNA synthesis. Although NuMA is insoluble in uninfected interphase cells, HSV infection induced solubilisation and dynamic relocalisation of NuMA, whereupon the protein became excluded from viral replication compartments – sites of virus transcription and replication. Live cell, confocal imaging showed that NuMA localisation dramatically changed from the early stages (diffusely nuclear, excluding nucleoli) to late stages of infection (central diminuition, but remaining near the inner nuclear peripheries). In addition, NuMA knockdown using siRNA suggested that NuMA is important for efficient viral growth. In summary, we suggest that NuMA is required for efficient HSV infection, and identify further areas of research that address how the virus challenges host cell barriers.

Supplementary material available online at
http://jcs.biologists.org/cgi/content/full/121/12/2087/DC1

Key words: Nuclear mitotic apparatus protein, Herpes simplex virus, Nuclear matrix, Live cell imaging

Introduction

The nuclear mitotic apparatus (NuMA) protein is a large, 236 kDa coiled-coil protein and an important component of the nuclear matrix in interphase cells (Sun and Schatten, 2006). NuMA is essential for spindle-pole organisation (Compton and Cleveland, 1994; Cleveland, 1995) and concentrates at the polar ends of the mitotic spindle (Lyderson and Pettijohn, 1980; Price and Petiijohn, 1986; Compton et al., 1992; Kallajoki et al., 1991; Toussen et al., 1991; Yang et al., 1992; Maekawa et al., 1991). Early in mitosis, after the breakdown of the nuclear envelope, NuMA is phosphorylated, solubilised and dispersed into the cytoplasm where it forms a complex with cytoplasmic dynein and dynactin, and translocates along microtubules to the spindle poles (Merdes et al., 1996; Merdes et al., 2000). Although many studies have shown diverse roles of NuMA, little is known about the role of NuMA in interphase cells (Sun and Schatten, 2006).

Herpes simplex virus (HSV) is a large DNA virus. After HSV infection, capsids are transported to nuclear pores through which the viral genome is released into the nucleus. After replication in the host cell nucleus, viral DNA is incorporated into preformed capsids (reviewed in Mettenleiter, 2004). The export of capsids through the nuclear membrane requires modification and reorganisation of nuclear membrane proteins. The nuclear membrane is prone to major morphological changes in HSV type 1 (HSV-1)-infected cells (Scott and O'Hare, 2001). In addition, phosphorylation of lamins and emerin in HSV-infected cells is thought to alter the nuclear membrane meshwork and facilitate capsid egress into the cytoplasm (Morris et al., 2007; Leach et al., 2007). The virally encoded UL31 and UL34 proteins, which target the inner nuclear membrane, are required for nucleocapsid envelopment, modification of nuclear structure and efficient cytoplasmic egress of capsids (Yamauchi et al., 2001; Reynolds et al., 2001; Reynolds et al., 2002; Fuchs et al., 2002; Simpson-Holley et al., 2004; Simpson-Holley et al., 2005; Klupp et al., 2007). The viral US3 protein kinase and cellular protein kinases are also important factors in modifying the nuclear structure (Muranyi et al., 2002; Simpson-Holley et al., 2004; Reynolds et al., 2004; Simpson-Holley et al., 2005; Park and Baines, 2006; Bjerke and Roller, 2006; Mou et al., 2007). During HSV infection, the nucleus expands (Simpson-Holley et al., 2005), suggesting that nuclear matrix proteins, which compose the nuclear framework, are regulated by the virus. However, it is still unknown how the virus mediates nuclear reorganisation.

Eukaryotic nuclei are responsible for complex and vital functions in interphase cells, such as DNA replication, and RNA transcription and processing. The nuclear structure temporally and spatially coordinates these processes, as highly condensed chromatin that is organised into discrete loops is attached to a nonchromatin scaffold that has been referred to as the nuclear matrix or nucleoskeleton (Gueth-Hallonet et al., 1998). NuMA is a highly insoluble nuclear matrix component that binds chromatin during interphase, disperses into the cytoplasm at the onset of mitosis, and finally redistributes to spindle poles in mitosis. In the earlier phases of HSV infection, the nuclear matrix may serve as a scaffold for capsid formation and viral DNA replication. Once the capsids have acquired viral DNA (encapsidation), they are destined for the cytosol. By contrast, the primary insolubility and rigidity of the nuclear matrix may hinder viral exit. It is possible that HSV and other herpes viruses have

evolved strategies to remodel the nucleus to enhance their replication.

Here, we show that NuMA is extensively phosphorylated and solubilised in HSV-infected cells. The formation of nuclear viral replication compartments coincided with the predominant exclusion of NuMA from these sites and the accumulation of NuMA at the inner nuclear periphery. Moreover, the dynamic change in NuMA localisation was delayed by PAA, a viral DNA polymerase inhibitor, suggesting that viral DNA synthesis and/or viral γ_2 protein synthesis were associated with this process. Finally, NuMA knockdown using small interfering RNA (siRNA) reduced viral replication, cell-to-cell spread, and egress into the extracellular space. Our study suggests that HSV targets NuMA and alters the nuclear structure of infected cells to facilitate viral replication.

Results

NuMA is phosphorylated in HSV-infected cells

NuMA is extensively modified by Cdc2 and tankyrase-1 in mitotic cells (Compton and Luo, 1995; Chang et al., 2005). To determine whether NuMA is modified in HSV-infected cells, HEp-2 cells were infected with HSV-1 or HSV-2 at a multiplicity of infection (MOI) of three plaque-forming units (PFU) per cell. Cells were harvested at various intervals and subjected to SDS-PAGE and western blotting for NuMA (Fig. 1A). NuMA motility gradually decreased as infection proceeded. This effect was observed earlier and to a greater extent in HSV-2-infected cells (Fig. 1A, lanes 1-4) than in HSV-1-infected cells (Fig. 1A, lanes 5-6), suggesting that modification of NuMA took place. The motility of the NuMA band was slower than that of mitotic cell extracts (not shown).

It is known that NuMA has many consensus sites for phosphorylation by protein kinases, especially in its C-terminus (Yang et al., 1992). To examine whether the modification of NuMA was due to phosphorylation, uninfected and infected cell samples were subjected to dephosphorylation with λ-phosphatase (Fig. 1B). Phosphatase digestion of extracts from HSV-2-infected cells resulted in a faster migrating NuMA (Fig. 1B, lane 4), indicating that the modification of NuMA was due to phosphorylation during HSV infection. Infection in the presence of the PARP inhibitor 3-aminobenzamide, which blocks tankyrase activity, did not interfere with the modification of NuMA in infected cells (data not shown).

NuMA phosphorylation is affected by a block in viral DNA synthesis

Phosphonoacetic acid (PAA) is a potent inhibitor of the HSV polymerase and thus inhibits viral DNA synthesis. Inhibition of viral DNA synthesis decreases the production of viral late γ_1 proteins and blocks the synthesis of γ_2 proteins. We examined the effect of PAA on NuMA modification. PAA treatment resulted in a faster migrating NuMA band (Fig. 1C, lane 3) compared with normally infected cells (Fig. 1C, lane 2) at 17 hours post infection. NuMA migration in PAA-treated cells was slower than in uninfected cells (Fig. 1C, lanes 1, 4) and indicated that NuMA modification did not occur so efficiently in the presence of PAA.

There are many phosphorylation sites in the C-terminus of NuMA. Cdc2 kinase sites located at Thr2000, Thr2040 and Ser2072 have been reported to be particularly important for NuMA to localise at spindles during mitosis and for the completion of cell division (Compton and Luo, 1995). As Cdc2 kinase activity is upregulated in HSV-infected cells (Advani et al., 2001), we examined whether these Cdc2 sites are responsible for NuMA phosphorylation in HSV-infected cells. We constructed plasmids that expressed full-length

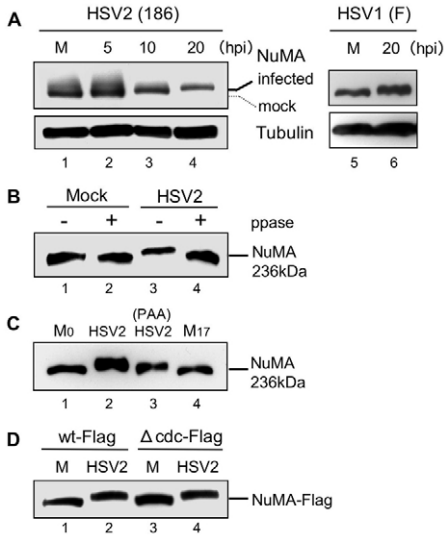

Fig. 1. (A) Extensive modification of NuMA in HSV-infected cells. HEp-2 cells infected with HSV-2 or HSV-1 at a MOI of 3 PFU/cell were harvested at the indicated time points and analysed by SDS-PAGE and western blotting with a NuMA polyclonal antibody. The slower migrating band is prominent at later times post infection. (B) NuMA is phosphorylated in HSV-infected cells. Uninfected HEp-2 cells (lanes 1, 2) or HEp-2 cells infected for 17 hours with HSV-2 at a MOI of 5 PFU/cell (lanes 3, 4) were harvested and dephosphorylated with λphosphatase (+) or incubated without phosphatase (–). NuMA in HSV-2-infected cells was phosphorylated (lane 3) and phosphatase treatment resulted in a faster migrating band (lane 4). (C) Blockage of viral DNA synthesis by PAA treatment reduces modification of NuMA in HSV-2-infected cells. HEp-2 cells were infected with HSV-2 at a MOI of 5 PFU/cell in the absence (lane 2) or presence (lane 3) of 300 μg/ml PAA and harvested at 17 hours post infection. Mock-infected cells were harvested before infection (lane 1) and also 17 hours later (lane 4). (D) The Cdc2 consensus sites in the C-terminal region of NuMA (Thr2000, Thr2040 and Ser2072) are not modified in HSV-2-infected cells. HEp-2 cells were transfected with pFLAG-NuMAwt and pFLAG-NuMAΔcdc2 and 24 hours later were mock-infected (lanes 1, 3) or infected with HSV-2 at a MOI of 3 PFU/cell for 15 hours (lanes 2, 4). The cells were harvested and analysed by SDS-PAGE and western blotting with an anti-FLAG monoclonal antibody. The motility of the bands in lanes 2 and 4 are nearly identical, suggesting that NuMA was not modified at the Cdc2 sites.

NuMA-FLAG and NuMAΔcdc-FLAG. At 20-24 hours after transfection, cells were infected with HSV-2 at a MOI of 3 PFU/cell. Migration of the FLAG fusion protein was detected with an anti-FLAG monoclonal antibody 15 hours post infection. Compared with non-infected cells, migration of NuMA-FLAG and NuMAΔcdc-FLAG was considerably slower in infected cells, indicating that the FLAG fusion did not interfere with NuMA modification. However, the migration of the two species was identical, suggesting that the Cdc2 sites were not phosphorylated (at least extensively) in infected cells.

NuMA is relocalised in HSV-infected cells

Having shown that NuMA is modified in HSV-infected cells, we next examined the intracellular localisation of the protein (Fig. 2). HEp-2 cells were infected with HSV-1, fixed at 3-hour intervals, and then analysed for NuMA localisation by indirect immunofluorescence with an anti-NuMA polyclonal antibody (Fig. 2A-F). NuMA is an exclusively nuclear protein in interphase cells (Yang et al., 1992) and was diffusely localised in the nucleus in uninfected cells (Fig. 2A). However, as infection progressed NuMA decreased in the central parts of the nucleus, whereas NuMA

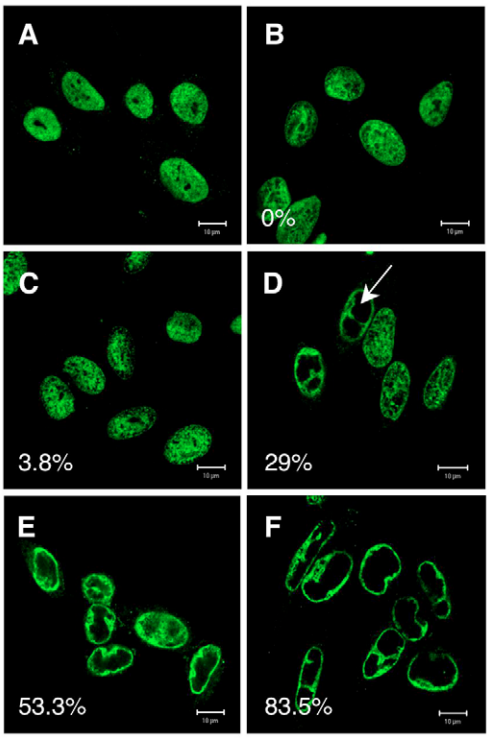

Fig. 2. (A-F) NuMA is relocalised in HSV-1-infected cells. HEp-2 cells were either mock-infected (A) or infected with HSV-1 at a MOI of 3 PFU/cell, fixed at 3 hours (B), 6 hours (C), 9 hours (D), 12 (E) and 15 hours (F) post infection, and then analysed for NuMA localisation. NuMA diminuition in the centre of the nucleus can be observed from 9 hours post infection (D). The percentage of cells exhibiting such nuclear localisation of NuMA (arrow in panel D) were quantified by examining at least 200 cells (given at bottom left within each panel).

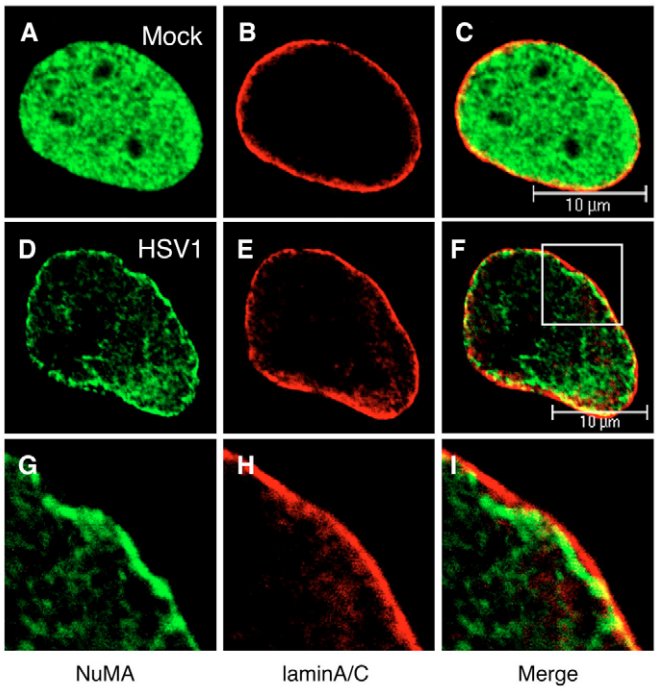

Fig. 3. (A-I) Comparison of the localisation of NuMA and lamin A/C. In mock-infected HEp-2 cells, NuMA was diffusely distributed throughout the nucleus excluding nucleoli (A) and surrounded by the nuclear membrane protein, lamin A/C (B,C). In cells infected for 15 hours with HSV-1, NuMA formed a ring-like structure similar to that of lamin A/C (D-F). However, magnification of the inner rims of the nucleus showed that the two proteins did not necessarily colocalise (G-I) and that NuMA was located on the inner nuclear side of lamin A/C.

increased at the inner rims of the nucleus (Fig. 2D-F). At late times post infection, infected cells exhibited a nuclear ring-like localisation of NuMA (Fig. 2F). For each time point, the percentage of cells that showed such reorganisation of NuMA in the whole cell population was quantified. The ring-like patterns of NuMA became eminent at around 9 hours post infection and the percentage of such cells rose steadily thereafter, reaching near 100% at later time points (e.g. 20 hours post infection). Thus, in HSV-infected cells, the localisation of the nuclear matrix protein NuMA was strikingly altered.

Furthermore, we compared the localisation of NuMA with that of the nuclear membrane protein lamin A/C (Fig. 3). In mock-infected cells, the outer boundaries of NuMA slightly overlapped with those of lamin A/C (Fig. 3A-C). In HSV-1-infected cells, NuMA was predominantly at the inner nuclear peripheries, touching the inner nuclear membrane (Fig. 3D-F). A detailed examination of the nuclear rim showed that, although NuMA composed a ring-like structure, the majority of the protein was located adjacent to or on the inner side of lamin A/C (Fig. 3G-I).

The localisation of NuMA and viral replication compartments are mutually exclusive

We further compared NuMA localisation with that of viral proteins. 14R-VP16G is a wild-type HSV-1 virus that encodes VP16, the major tegument protein, fused to GFP and replicates normally in cultured HEp-2 cells (Yamauchi et al., 2008). HEp-2 cells were infected with 14R-VP16G at a MOI of 1 PFU/cell and fixed 8 hours post infection. We found that VP16-GFP and NuMA localised to mutually exclusive regions in the nucleus (Fig. 4A-C). We also examined the localisation of VP16-GFP, NuMA and another tegument protein, UL17, which functions in viral DNA cleavage and packaging (Fig. 4D-G). VP16-GFP and UL17 colocalised in the nucleus and NuMA antigenicity was reduced in these places, suggesting a correlation between NuMA localisation and the formation of nuclear viral replication factories. We confirmed the localisation of replication compartments by staining with ICP8, the single strand (ss)-DNA-binding protein. Replication compartments can be categorised into stages I-IV, based on the progress of infection (Burkham et al., 1998). At 12 hours post HSV-1 infection, NuMA and replication compartments exhibited mutual exclusion (stage IV, Fig. 4I-K).

NuMA is solubilised in HSV-infected cells

Herpes viruses are known to solubilise nuclear structural proteins as a strategy to overcome physical nuclear barriers (Muranyi et al., 2002; Mou et al., 2007). We examined whether infection affected the solubility of NuMA, an otherwise insoluble component of the nuclear matrix in interphase cells. HEp-2 cells or HEp-2 cells that transiently express NuMA-FLAG were mock-infected or infected with HSV-1 at a MOI of 3 PFU/cell. At 15 hours post infection, cells were pre-extracted, fixed, and analysed by indirect immunofluorescence for NuMA. Both NuMA (Fig. 5A) and NuMA-FLAG (Fig. 5C) were diffusely nuclear in mock-infected cells

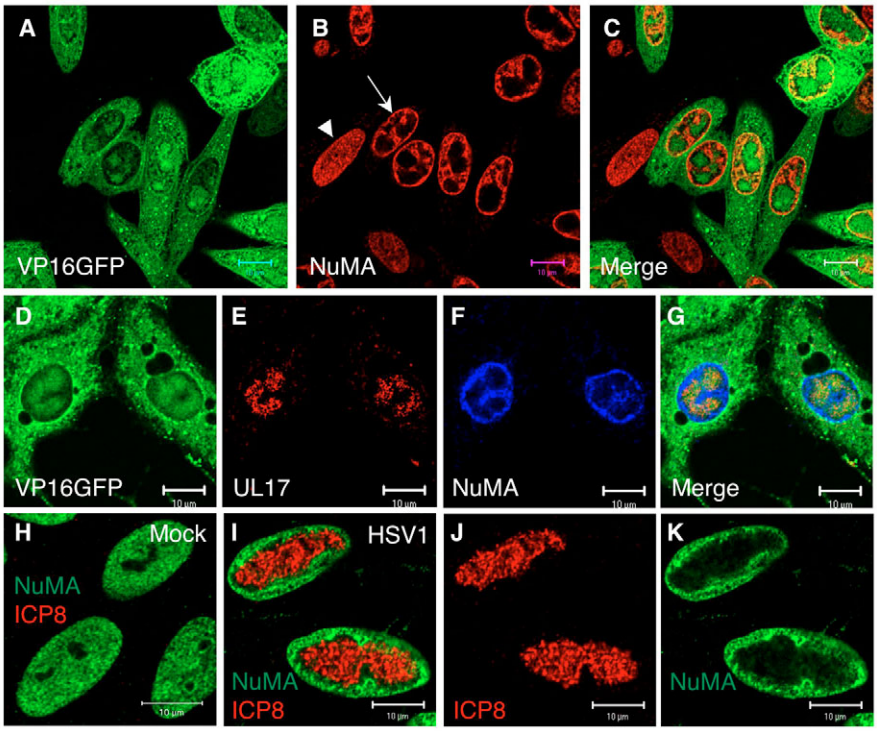

Fig. 4. NuMA and its relation to viral proteins and replication compartments. (A-C) HEp-2 cells were infected with 14R-VP16G at a MOI of 1 PFU/cell. Cells were fixed at 8 hours post infection and analysed for VP16-GFP and NuMA by indirect immunofluorescence. VP16-GFP (A) and NuMA (B) localised almost exclusively of each other. Note the difference in NuMA localisation between an uninfected cell (arrowhead) and an infected cell (arrow) (B). (D-G) Further analysis with triple fluorescence of VP16-GFP (D), UL17 (a tegument protein) (E) and NuMA (F) showed that, whereas the two viral proteins colocalised in the nucleus, NuMA localisation excluded these proteins. Analysis of NuMA and ICP8 localisation in mock-infected (H) and infected cells (I-K). Cells were infected with HSV-1 at a MOI of 3 PFU/cell and then fixed at 12 hours post infection. NuMA and ICP8 (a marker for replication compartments) exhibited mutually exclusive localisation.

reflecting their insolubility. However, at 15 hours post infection, the fluorescence in the nucleus decreased considerably, suggesting that the majority of NuMA (Fig. 5B) and NuMA-FLAG (Fig. 5D) were solubilised. We confirmed this observation by cell fractionation. HEp-2 cells were either mock-infected or infected with HSV-2 at a MOI of 3 PFU/cell in the absence or presence of PAA. At 15 hours post infection, cells were harvested and submitted to cell fractionation and separated into insoluble pellets (P) and soluble (S) fractions. The fractions were analysed by SDS-PAGE and western blotting for NuMA, the major capsid protein VP5, lamin A/C and calnexin (Fig. 5E). Although NuMA was largely insoluble in uninfected cells, its soluble fraction increased substantially in infected cells. However, in the presence of PAA, the insolubility of NuMA was similar to mock-infected cells. In addition, the soluble fraction of lamin A/C also increased under normal infection conditions, which is consistent with data shown by others (Reynolds et al., 2004). In addition, the expression of VP5 (a γ_1 protein) was considerably reduced in PAA-treated cells.

Examination of NuMA dynamics in live cells

The next experiment assessed the relationship between viral protein accumulation and NuMA localisation in more detail. To visualise viral replication in live cells, we used the HSV-1, F-VP26/GFP virus, which encodes the minor capsid protein, VP26, fused to GFP (Snyder et al., 2006). To visualise NuMA, we constructed pcmRFP-NuMA, which expresses full-length NuMA with an N-terminal monomeric RFP. Vero cells were transfected with pcmRFP-NuMA and infected with F-VP26/GFP at a MOI of 5 PFU/cell 20-24 hours post-transfection. Laser confocal images were obtained from the bottom to the top of the cell (about 20 planes) every 10 minutes. Each slice was projected into a single image that displayed all of the fluorescence detected in the cell.

Viral protein accumulation

This examination (Fig. 6, supplementary material Figs S1, S2 and Movie 1) showed that NuMA localisation began to change around

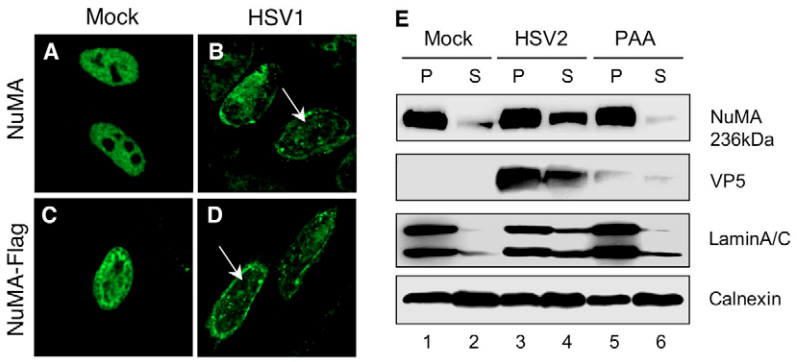

Fig. 5. Solubilisation of NuMA by HSV infection. HEp-2 cells (A,B) or HEp-2 cells transiently expressing NuMA-FLAG (C,D) were either mock-infected or infected with HSV-1 at a MOI of 3 PFU/cell. Twenty hours later, the cells were pre-extracted with 0.1% Triton X-100, fixed, and analysed by indirect immunofluorescence using an anti-NuMA polyclonal antibody (A,B) or anti-FLAG monoclonal antibody (C,D). In mock-infected cells, both NuMA proteins were resistant to extraction with Triton X-100 (A,C). In infected cells, the majority of NuMA and NuMA-FLAG were extracted except for that in the inner nuclear rims and subtle intranuclear foci (B,D), suggesting that NuMA was extensively solubilised. (E) NuMA is solubilised in infected cells and solubilisation is suppressed by PAA. HEp-2 cells were either mock infected (lanes 1, 2) or infected with HSV-2 at a MOI of 3 PFU/cell in the absence (lanes 3, 4) or presence (lanes 5, 6) of PAA. At 15 hours post infection, cells were fractionated, and resulting insoluble (P) and soluble (S) fractions were subjected to SDS-PAGE and western blotting. The blot was detected for NuMA, the major capsid protein VP5, lamin A/C and calnexin (loading control). The soluble fraction of NuMA and lamin A/C increased upon infection. Inhibition of viral DNA synthesis had a suppressive effect on the solubilisation of these proteins. VP5 expression was greatly reduced upon PAA treatment.

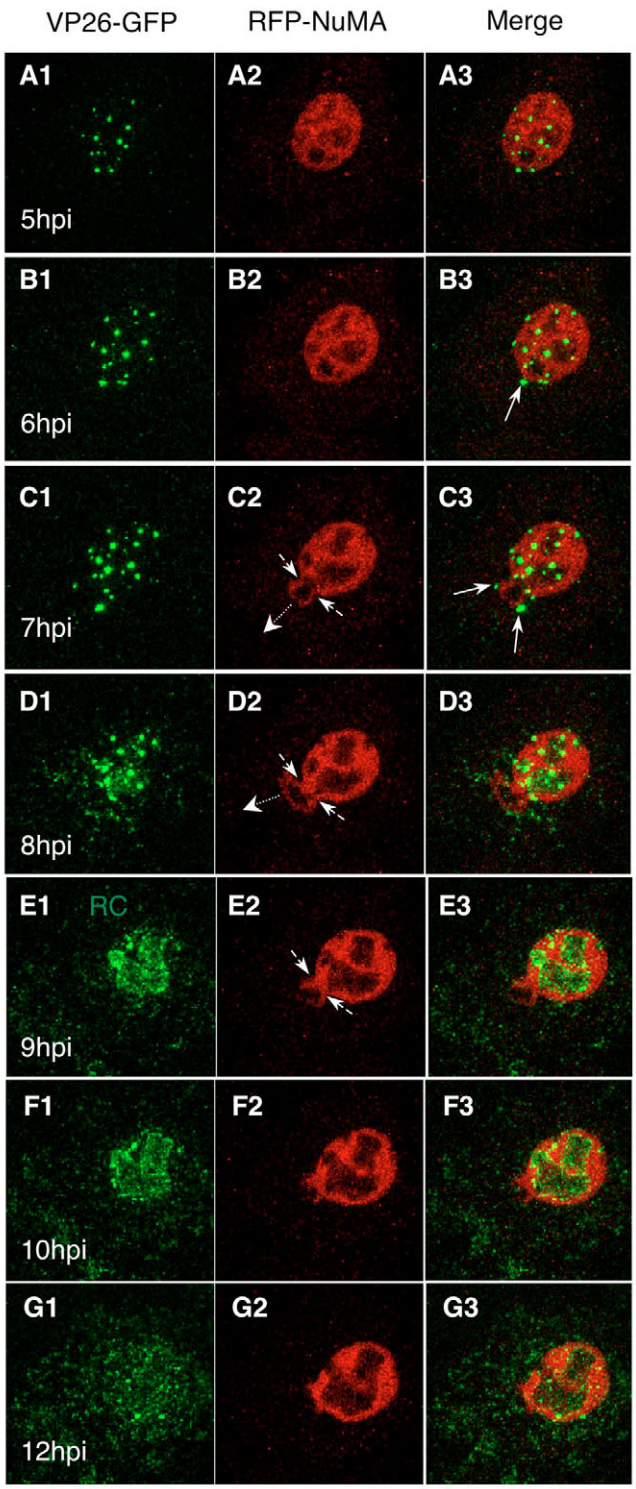

Fig. 6. Live cell, time-lapse photographs of Vero cells transiently expressing RFP-NuMA and infected with F-VP26/GFP at a MOI of 5 PFU/cell (5-12 hours post infection). Individual panels were projected from 20-25 *z*-axes, confocal sections to represent the total fluorescence in the cell. RFP-NuMA began to decrease in the central parts of the nucleus where the initial accumulation of VP26-GFP was observed (A,B). The solid-lined arrows in B3 and C3 show foci of potential primary enveloped capsids whose egress into the cytoplasm was accompanied by a contortion of the nucleus (C2,D2,E2: dotted-lined arrows) and a pushing-out of the nucleus into the direction of the cytoplasm (C2,D2: fine dotted-lined arrows). Replication compartments (RC, E1) formed most readily in places comparatively void of RFP-NuMA (E3,F3). At late times post infection, the overall RFP-NuMA distribution did not change and remained mostly in a ring-like pattern (G2) while VP26-GFP was dispersed in the cytoplasm (G1). At times later than 15 hours, VP26-GFP in progeny virions was found also in the extracellular space (see supplementary material Movie 1).

4 to 6 hours post infection, when hollows in the central areas of RFP-NuMA gradually enlarged. The discrete nuclear foci of VP26-GFP often formed near or on the inner edges of these NuMA-less places (Fig. 6A1-A3,B1-B3). In general, the majority of VP26-GFP and RFP-NuMA did not colocalise; the yellow colour in the merged pictures were mostly found at the inner rims of the hollows of RFP-NuMA (Fig. 6, and supplementary material Fig. S1).

Capsid maturation, formation of replication compartments, and potential egress of capsids from the nucleus into the cytoplasm

Occasionally, rather large VP26-GFP foci (potential C-capsids or DNA-containing capsids) were seen exiting from the nucleoplasm into the cytoplasm around 7-10 hours post infection (Fig. 6C3,D3). It is possible that these comparatively large foci (Fig. 6B3,C3, arrows) represent a cluster of primary enveloped capsids (or capsids prior to becoming primary enveloped) in the perinuclear space between the inner and outer nuclear membranes (or just inside the inner nuclear membrane). In some cells this reproducible phenomenon was accompanied by a contortion of the nucleus near the potential sites of exit (Fig. 6C2,D2,E2, arrows). (It is possible that this nuclear morphological change is either directly or indirectly caused by the overexpression of RFP-NuMA. However, this change was observed repeatedly and was usually accompanied by dispersion of VP26-GFP into the cytoplasm.) At the same time as capsid dispersal, VP26-GFP formed a globular structure in the nucleus (replication compartment) in the hollow or faint regions of RFP-NuMA (Fig. 6E1-E3,F1-F3), which supports our previous observations (Fig. 3). After the bulk of capsids dispersed into the cytoplasm, the aberrantly shaped nucleus gradually changed (or some of the nucleus collapsed into the cytoplasm probably owing to physical weakness) into the more normal spherical shape (Fig. 6F2-G2).

Progeny virus production and extracellular egress

After the initial accumulation of VP26-GFP in replication compartments, the majority of the GFP fluorescence was distributed throughout the cell and extracellularly in infectious progeny virions. Less change in localisation was observable in RFP-NuMA, typically after 12 hours post infection (Fig. 6G2, and supplementary material Movie 1 for later time points), representative of the ring-like fixed-cell images shown earlier (Fig. 2F). These observations confirmed that dynamic relocalisation of NuMA inside the nucleus during HSV infection is concurrent with viral protein accumulation. The redistribution of RFP-NuMAΔcdc and RFP-NuMA was essentially the same in HSV-1-infected cells (data not shown).

Reorganisation of NuMA is inhibited by a block of viral DNA synthesis

Phosphonoacetic acid (PAA) inhibits HSV DNA polymerase. We showed that PAA decreased NuMA phosphorylation and solubilisation in HSV-infected cells (Fig. 1C, Fig. 5E). As replication

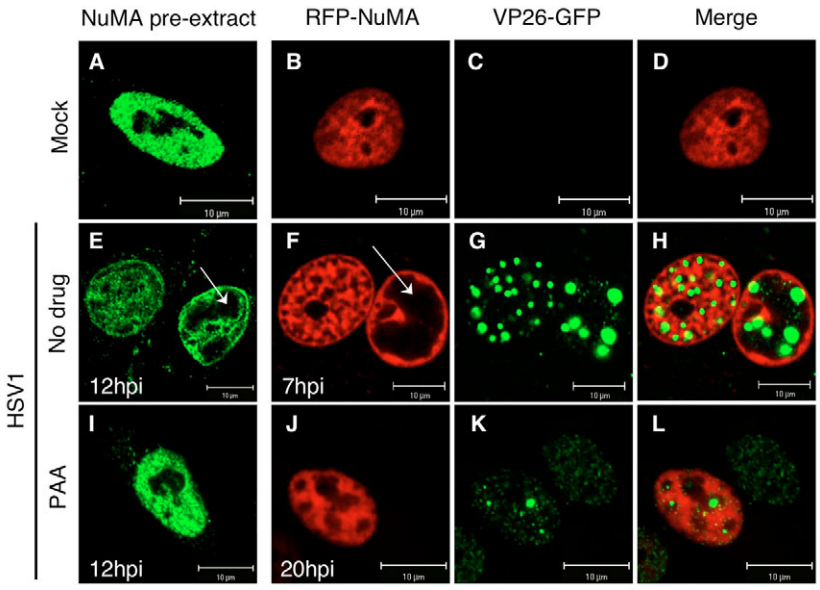

Fig. 7. The hollowing of NuMA is blocked by PAA. HEp-2 cells mock infected (A) or infected with HSV-1 in the absence (E) or presence (I) of PAA were pre-extracted with 0.1% Triton X-100 prior to fixation at 12 hours post infection. hollowing of NuMA was observed in normal, infected cells (arrow) (E). In cells infected in the presence of PAA, the localisation of NuMA (I) was the same as that in mock-infected cells (A), suggesting that viral DNA synthesis was important for the relocalisation and solubilisation of NuMA. In Vero cells that were transiently transfected with RFP-NuMA, infected with F-VP26/GFP, and then fixed at 7 hours post infection, the centre of the nucleus (where VP26-GFP had accumulated) lacked RFP-NuMA (F-H). In PAA-treated infected cells, however, the pattern of RFP-NuMA was similar to uninfected cells (B-D) at 7 hours post infection (data not shown). Even at 20 hours post infection, most of RFP-NuMA remained in the central parts of the nucleus (J-L).

compartments are sites of transcription and DNA replication, we examined whether viral DNA synthesis was involved in the reorganisation of NuMA in infected cells. HEp-2 cells were infected with HSV-1 and incubated with or without PAA from 1 hour post infection. At 12 hours post infection, prior to fixation, cells were extracted and NuMA localisation was examined by indirect immunofluorescence (Fig. 7A,E,I). Strikingly, the decrease of nuclear NuMA observed in normal, infected cells (Fig. 7E, arrow) was abrogated completely in all cells in the presence of PAA (Fig. 7I). This indicated that viral DNA synthesis, γ_2 protein synthesis (which depends on viral DNA synthesis) and/or NuMA phosphorylation are involved in NuMA solubilisation and relocalisation.

In addition, Vero cells that transiently express RFP-NuMA were infected with F-VP26/GFP at a MOI of 5 PFU/ml in the presence or absence of PAA. The decrease in RFP-NuMA was observed at 7 hours post infection (Fig. 7F, arrow). At 7 hours post infection in the presence of PAA, RFP-NuMA localisation (data not shown) was similar to that in mock-infected cells (Fig. 7B-D). At 20 hours post infection, there was leaky VP26-GFP expression and a slight loss of NuMA fluorescence from the centre of the nucleus (Fig. 7J-L). This indicated that viral DNA synthesis was a key factor in NuMA redistribution in HSV-infected cells.

Effects of actin-disrupting drugs on the reorganisation of NuMA in HSV-infected cells

G-actin is a monomeric form of actin that has been proposed to exist in the nucleus (Pederson and Aebi, 2002). Pseudorabies virus, an α-herpes virus, induces the formation of nuclear actin filaments (Feierbach et al., 2006). In HSV-1-infected cells, disruption of G-actin decreased capsid movement rates (Forest et al., 2005) and prevented certain changes in nuclear architecture induced by the virus without affecting viral growth (Simpson-Holley et al., 2005). We examined whether inhibitors of F-actin (cytochalasin D) and G-actin (latrunculin A) affected the reorganisation of NuMA. HEp-2 cells were infected with HSV-1 in the presence of 2.5 μM cytochalasin D, 1 μM latrunculin A or (as control) the solvent DMSO. The cells were fixed 10 hours post infection and NuMA was examined by indirect immunofluorescence (Fig. 8). Loss of NuMA fluorescence from the centre of nuclei was observed in cells treated with DMSO (Fig. 8A-C) and, to a slightly lesser extent, in those treated with cytochalasin D (Fig. 8E-G). In cells treated with latrunculin A, diminuition was not blocked, although its area was considerably decreased compared with DMSO-treated cells (Fig. 8I-K). When infected cells were quantified for such relocalisation of NuMA, both cytochalasin-D- and latrunculin-A-treated cells showed similar values. We further examined the relationship of NuMA with replication compartments in the presence of these drugs (Fig. 8D,H,L). The results showed that disruption of G-actin affected the formation and/or maturation of replication compartments (Simpson-Holley et al., 2005), but did not affect the exclusion of NuMA from the replication compartments (Fig. 8L). Therefore, the redistribution of NuMA in infected cells does not dependent on G-actin function. In addition, viral growth was not greatly affected by these drugs (data not shown).

Knockdown of NuMA by siRNA debilitates viral growth, especially at low MOI values

We examined the effect of NuMA knockdown on the efficiency of viral growth. NuMA has been reported to be non-essential for the formation of the nucleus (Merdes and Cleveland, 1997). HEp-2 cells were transfected with siRNA targeting NuMA (siNuMA) or control siRNA (siCont) and knockdown efficiency was analysed by western blotting. NuMA expression was efficiently reduced in siNuMA-transfected cells 3 days after transfection, whereas lamin B and actin expression were not affected (Fig. 9A). As reported by others, some of the siNuMA-transfected cells exhibited apoptotic characteristics and growth arrest (Harborth et al., 2001). At 3 days post transfection, siNuMA-treated cells had on average 75% viability compared with control cells, as determined by Trypan-Blue exclusion (data not shown).

We analysed the cell-to-cell spread of 14R-VP16G virus that was infected at a low MOI (0.001 PFU/cell) 3 days after transfection of siRNAs. The cells were fixed 48 hours post infection and examined for VP16-GFP fluorescence to assess viral spread. siNuMA-transfected cells (Fig. 9E-G) showed considerably slower viral spread than control cells (Fig. 9B-D), suggesting that NuMA knockdown slowed viral growth. The average diameters of 14R-

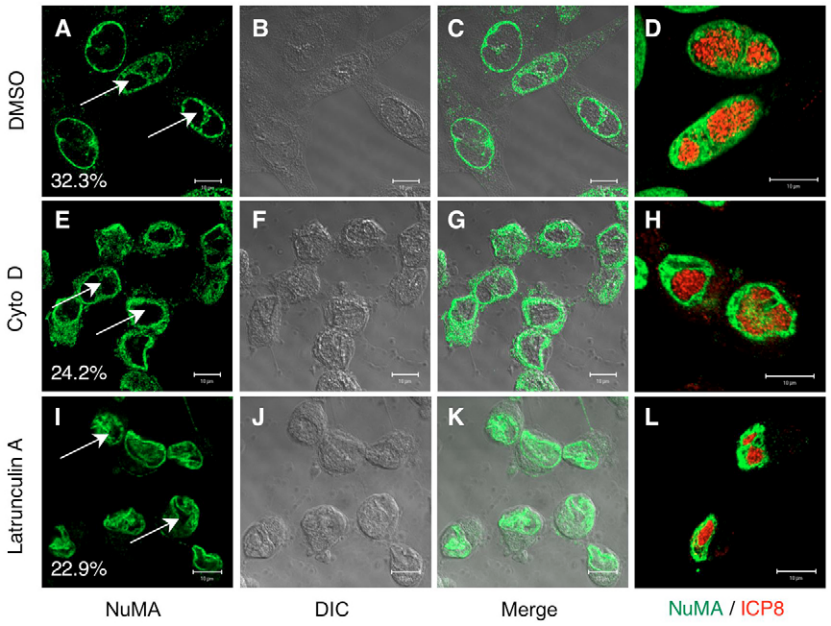

Fig. 8. Disruption of G-actin or F-actin does not affect the exclusion of NuMA from replication compartments. HEp-2 cells were infected with HSV-1 at a MOI of 3 PFU/cell and after 1 hour, cultured in the presence of the solvent DMSO (A-D), cytochalasin D (E-H) or latrunculin A (I-L). At 10 hours post infection, the cells were fixed and analysed for NuMA or NuMA/ICP8 localisation. DMSO-treated cells showed the typical decrease in NuMA inside the nucleus as shown by the arrows (A-C) and its exclusion from replication compartments (D). Cytochalasin D, which disrupts F-actin, slightly affected nuclear morphology but exhibited the representative NuMA pattern as shown by the arrows (E-G,H). Latrunculin A, which inhibits G-actin, affected the size of both replication compartments and NuMA-void areas (I-K,L). The arrows in panel I show that decrease of NuMA fluorescence was constricted to much smaller areas. The percentage of cells exhibiting such NuMA relocalisation were quantified (in at least 200 cells) and shown in panels A,E,I.

VP16G plaques in siNuMA- and siCont-transfected cells were 247 μM and 96 μM, respectively (P<0.001; Student's t-test) (Fig. 9H). All of the plaques observed were uniformly smaller in siNuMA-treated cells compared with control cells. To analyse the growth of HSV-1 in detail, siRNA-treated HEp-2 cells were infected with HSV-1 at a MOI of 0.01 PFU/cell. The infected cells were harvested at various time points to obtain a time course for virus yield. In addition, the viral yield of siNuMA- and siCont-treated cells were normalised to PFU/ml per 10^6 cells. A representative multi-step growth curve showed that NuMA expression was important for efficient growth at a low MOI (Fig. 9I). The reduction in overall viral yield was ~50-100 fold, depending on the experiment. In addition, NuMA knockdown suppressed one-step viral growth and extracellular egress of viral particles when infected at a higher MOI of 3 PFU/cell, such that the average viral yield at 24 hours post infection (n=2) was 4.2×10^8 and 3×10^7 PFU/ml for siCont- and siNuMA-treated cells, respectively (data not shown).

These observations suggested that NuMA knockdown affected efficient HSV replication. Whether this phenotype was the result of a specific defect in virus replication or a more global effect on the host cell because of NuMA deprivation is currently unknown. However, it is possible that NuMA knockdown induced a more quiescent state, as indicated by slower replication of siNuMA-treated cells, that is disadvantageous for HSV replication.

Discussion

When viruses infect mammalian cells, they often manipulate host-cell mechanisms to favour their replication. Insights into these viral 'takeovers' often help unravel unknown cellular functions. This study showed that HSV infection altered the kinetics of NuMA, a nuclear matrix component. Efficient egress of herpes viruses, including HSV, depends on concerted functions of viral and cellular proteins (reviewed in Mettenleiter, 2004). Recent findings have suggested that herpes viruses disrupt nuclear barriers by encoding specific proteins that target the nuclear membrane and by recruiting cellular proteins such as PKs to sites of nuclear remodeling (Yamauchi et al., 2001; Muranyi et al., 2002; Reynolds et al., 2004; Farina et al., 2005; Gonnella et al., 2005; Simpson-Holley et al., 2005; Bjerke and Roller, 2006; Park and Baines, 2006; Klupp et al., 2007; Leach et al., 2007; Morris et al., 2007; Mou et al., 2007). ND10 proteins are also disrupted upon HSV-1 infection and relocate to sites associated with viral genome complexes (Everett and Zafiropoulos, 2004; Everett and Murray, 2005). Our study is the first to demonstrate that NuMA is extensively modified in HSV-infected cells.

NuMA has been shown to undergo cell-cycle dependent phosphorylation and dephosphorylation that controls its distribution and function. The 220 kDa and 240 kDa proteins detected by western blotting are most likely to represent the hypophosphorylated interphase form and the hyperphosphorylated mitotic form of NuMA, respectively. In interphase cells, NuMA is predominantly nuclear and insoluble, and a possible nuclear structural component. Phosphorylated NuMA disperses into the cytoplasm during nuclear envelope breakdown but the NuMA kinases and phosphatases have not been identified. Hyperphosphorylation of NuMA by Cdc2 kinase appears to allow NuMA to associate with centrosomes and/or microtubules at the spindle poles (reviewed in Sun and Schatten, 2006). NuMA is also a major acceptor of poly(ADP-ribosylation) by tankyrase 1 in mitosis; however, the functional significance of this phenomenon is not clear (Chang et al., 2005; Compton, 2005).

In apoptotic cells, NuMA is a target of caspase cleavage and is redistributed prior to, or coincidently with, the onset of DNA degradation. Proteolysis of NuMA by caspases produces 180 kDa, 190 kDa and 160 kDa fragments, and leads to disintegration of the nuclear structure (reviewed in Sun and Schatten, 2006). NuMA and nuclear lamins are cleaved upon infection with human rhinovirus 1B or measles virus and are target proteins during virus-induced programmed cell death (Taimen et al., 2004). HSV infection triggers an apoptotic response that is blocked late in infection by the virus through the synthesis of anti-apoptotic proteins (reviewed in Nguyen and Blaho, 2007). The cleaved form of NuMA (180 kDa and 190 kDa) slightly increased during late stages of HSV infection (not shown). When cells were infected in the presence of the caspase inhibitor Z-VAD-FMK (50 μM), NuMA

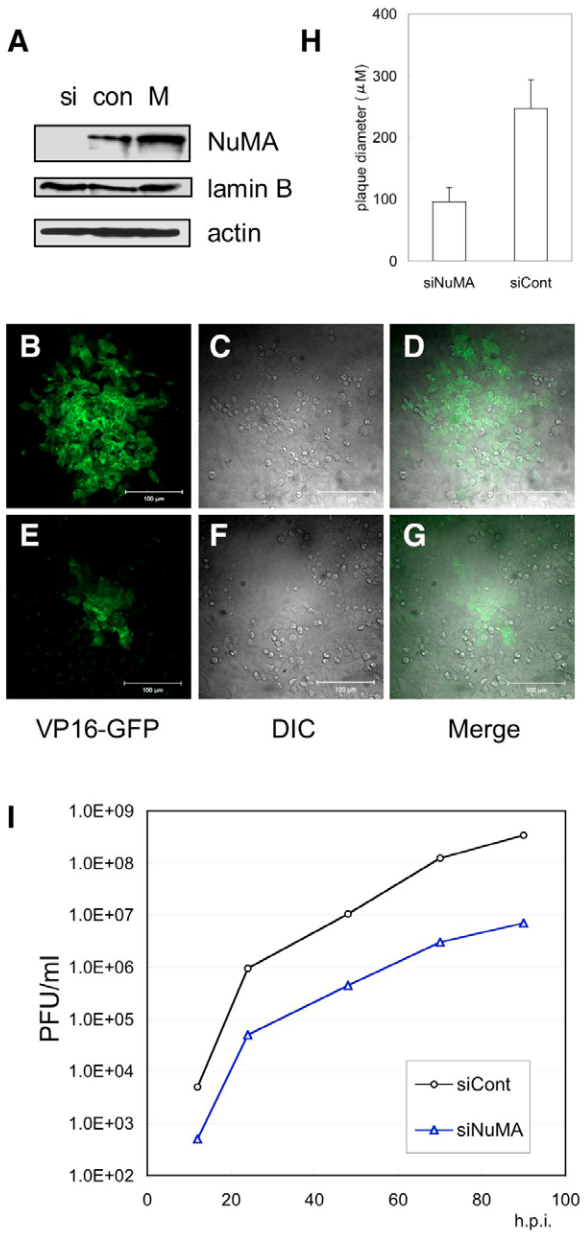

Fig. 9. NuMA knockdown using siRNA results in an HSV growth defect. (A) siNuMA-, siCont- or mock-transfected HEp-2 cells were analysed 3 days post-transfection for protein expression. NuMA levels were greatly decreased in siNuMA-transfected cells, whereas levels of lamin B and actin were constant. (B-G) Analysis of viral cell-to-cell growth in siRNA-treated cells. HEp-2 cells transfected with siCont (B,C,D) or siNuMA (E,F,G) were infected with 14R-VP16G at a MOI of 0.001 PFU/cell, fixed at 48 hours post infection, and examined for VP16-GFP (B,E). DIC (C,F) and merged images (D,G) show that cell-to-cell viral spread was considerably affected in siNuMA-transfected cells and that this was not a consequence of low cell density. (H) Comparison of 14R-VP16G plaque diameters in siCont- and siNuMA-transfected cells. Cells were fixed at 48 hours post infection and 30 randomly chosen plaques were scanned with the confocal microscope followed by measurement of plaque diameter with the Zeiss LSM software. Error bars represent standard deviations. (I) A multi-step growth curve of HSV-1 in siRNA-treated HEp-2 cells. The results shown are representative of three independent experiments. After similar treatment with siRNA, HEp-2 cells were infected with HSV-1 at a MOI of 0.01 PFU/cell. Cells were harvested at various times post infection to obtain viral growth curves and the resulting viral yield was normalised to per 10^6 cell. Cells that were not transfected with siRNA showed similar growth kinetics as siCont-transfected cells (not shown). The viral growth kinetics were considerably hampered in NuMA knockdown cells.

cleavage was completely blocked (without affecting viral growth), whereas the characteristic loss of NuMA from the centre of the nucleus was readily observed (data not shown). This suggested that even though a small fraction of NuMA is cleaved by caspases in HSV-infected cells (especially late in infection), this is not the direct cause of the dynamic relocalisation of NuMA. Furthermore, NuMA relocalisation was observed as early as 5 hours post infection with live cell imaging, again suggesting that the redistribution is not caused by proteolytic cleavage of NuMA. Thus, it is unlikely that HSV-induced NuMA reorganisation is due to apoptosis-induced alterations in nuclear morphology, suggesting that the modification of NuMA is distinct from known mechanisms.

The dynamic changes of NuMA observed in HSV-infected cells were striking, in that efficient redistribution was dependent on viral DNA synthesis and concurrent with viral protein accumulation in the nucleus. NuMA was extensively phosphorylated in HSV-infected cells. Modification was more prominent (judged by the slower NuMA migration) in HSV-2-infected cells than in HSV-1-infected cells, the reason for which is unknown. The Cdc2 phosphorylation sites in NuMA are important for NuMA localisation to spindle poles and the correct completion of mitosis (Compton and Luo, 1995). In HSV-infected cells, however, NuMA was not phosphorylated at these sites. As NuMA has consensus sites for a number of protein kinases, such as cAMP-dependent protein kinase PKC, Cdc2 kinase and Ca^{2+}/calmodulin kinases (Yang et al., 1992), any one of a large number of sites in NuMA could be phosphorylated in HSV-infected cells. The C-terminal region of NuMA might be a good candidate for modification by HSV.

We also found that HSV-mediated alteration of NuMA localisation was dependent on the synthesis of viral DNA. Analysis of live Vero cells that express RFP-NuMA demonstrated that the accumulation of VP26 inside the nucleus coincided with NuMA relocalisation as early as 4-5 hours post infection. In general, the effects of infection were characterised by a hollowing at the centre of the nucleus with NuMA concentrating at the inner rims, exclusive of viral replication compartments. In addition, by examining RFP-NuMA dynamics, we unexpectedly observed contortion of the nucleus that appeared to coincide with the dispersal of nucleocapsids into the cytoplasm. Thus, NuMA can serve as a marker of HSV-induced morphological changes in the nucleus. However, the contortion of the nucleus was not observed in all of the cells that expressed RFP-NuMA, suggesting that such changes in nuclear morphology are not a requirement for virus replication. As NuMA is targeted for solubilisation under HSV-infection conditions, excess amount of the protein might have hindered smooth exit of capsids from the nucleus to the cytoplasm. It is also possible that the overexpression of NuMA resulted in a more rigid nuclear structure or a denser nuclear lattice that provided more obstacles for the virus.

In HSV-1-infected cells, disruption of monomeric G-actin by latrunculin A prevents nuclear expansion, chromatin fragmentation, and replication compartment maturation, whereas disruption of F-actin by cytochalasin has none of these effects (Simpson-Holley et al., 2005). The disruption of monomeric G-actin did not block NuMA reorganisation but the smaller replication compartments that had formed coincided with a decrease in the area in which NuMA antigenicity was reduced. Our study suggests that NuMA reorganisation is linked to nuclear expansion induced by HSV infection.

Knockdown of endogenous NuMA by siRNA effectively decreased viral growth, especially at low MOI values. This

reduction in viral growth may have occurred because NuMA served as a scaffold for initial HSV assembly, DNA replication, DNA encapsidation, capsid maturation etc., or because NuMA knocked down cells had entered a quiescent state that altered cellular mechanisms required for efficient viral growth. Using siRNA transfection, it might not be possible to deplete NuMA completely. Therefore, to assess the importance of NuMA modification during infection, it will be necessary to analyse cells that express a mutant NuMA that cannot be modified. Alternatively, identifying the virally encoded gene(s) that relocalises NuMA is equally important. These challenging issues are interesting topics for further investigation.

Materials and Methods

Cells and viruses

Cells of the immortalised African green monkey kidney cell line Vero, and the human larynx carcinoma cell line HEp-2, were propagated as described previously. The HSV-1 wild-type virus F and F-VP26/GFP were kind gifts from Bernard Roizman (University of Chicago, IL) and David Johnson (Oregon Health & Sciences University, Portland, OR), respectively. The VP16-GFP expressing HSV-1 wild-type virus, 14R-VP16G, (Yamauchi et al., 2008) and HSV-2 wild-type virus 186 were also used. Viral stocks were propagated and titrated on Vero cell monolayers.

Preparation of mitotic cells

Exponentially growing HEp-2 cells were supplemented with 250 μg/ml nocodazole and cultured for 12-15 hours, after which a large fraction of the cells were seized at mitosis. Mitotic cells were released into the culture medium by extensive agitation and shaking of the flasks (mitotic shake off) (Hsu and Yeh, 1996). The detached cells were harvested by centrifugation, washed and designated the mitotic fraction.

Phosphatase assays

HEp-2 cells infected for 15 to 16 hours with HSV at a multiplicity of infection (MOI) of five plaque-forming units (PFUs) per cell were washed in cold, sterile PBS and harvested in lysis buffer [50 mM Tris-HCl (pH 8), 150 mM NaCl, 1% NP40, 0.5% sodium deoxycholate (DOC), 2 mM EDTA, 1 mM DTT and protease inhibitor cocktail (Sigma)] on ice. After 10 minutes on ice, the lysates were centrifuged at 14,000 ***g*** for 10 minutes at 4°C and the supernatants were transferred to a fresh tube. Lysates were supplemented with phosphatase buffer and $MnCl_2$ and dephosphorylated with 2000 units of l phosphatase (NEB) for 30 minutes at 30°C. The reaction was terminated with 4× SDS sample buffer, boiled and analysed by SDS-5% PAGE and western blotting with an anti-NuMA polyclonal antibody.

Expression vectors

The plasmids encoding NuMA wild type , NuMA2000TA2040TA2072SA cDNAs (NuMAΔcdc2), and pcDNA3-EGFP-NuMA were kind gifts from Duane Compton (Dartmouth Medical School, Hanover, NH) and Andreas Merdes (Centre National de la Recherche Scientifique – Pierre Fabre, Toulouse, France), respectively. Monomeric RFP (provided by Roger Tsien, University of California at San Diego, La Jolla, CA) was PCR amplified using forward (F) and reverse (R) primers F (5′-GCGGATCCACCATGGCCTCCTCCG-3′) and R (5′-ATGAATTCGGCGCCGG-TGGAG-3′) and inserted into the pcDNA3.1(+) (Invitrogen) plasmid using restriction sites *Eco*RI and *Xba*I to generate the vector pcmRFP. NuMA wt and NuMAΔcdc2 were PCR amplified using primers F (5′-CGGAATTCACCATGACACTCCAC-3′) and R (5′-GCTCTAGATTAGTGCTTTGCCTT-3′) and inserted into pcmRFP using restriction sites *Eco*RI and *Xba*I. All PCRs were carried out using the Phusion polymerase (Finnzymes). RFP-NuMA wild type localised to spindle poles during mitosis and with nuclei in daughter cells (not shown), indicating that the mRFP fusion did not interfere with spindle pole formation. However, micronucleation was observed because of NuMA overexpression (not shown).

Cell fractionation

Uninfected or infected HEp-2 cells were washed once in sterile PBS, harvested and pelleted. The pellet was resuspended and lysed in PBS supplemented with protease inhibitor cocktail (Sigma) and 0.25% Triton X-100, left on ice for 5 minutes and centrifuged at 6,000 ***g*** for 10 minutes at 4°C. The resulting cell pellet (P) and supernatant (S) were separated and solubilised in an equal final volume of sample buffer.

Antibodies

The anti-NuMA polyclonal antibody was a kind gift from Duane Compton and also purchased from NOVUS. The anti-NuMA monoclonal antibody was obtained from Oncogene. The following other monoclonal antibodies were purchased: anti-lamin A/C (Chemicon), lamin B (Zymed), anti-FLAG (Sigma), anti-β actin, anti-tubulin, anti-VP5 (Abcam), anti-ICP8 (EastCoast Bio), anti-calnexin (Santa Cruz Biotechnology). The anti-UL17 polyclonal antibody has been described previously (Goshima et al., 2000).

Immunofluorescence

All procedures were performed as described previously (Yamauchi et al., 2008). Briefly, cells grown on coverslips were washed in PBS and then fixed in –20°C methanol for 10 minutes. For short-term storage, the fixed cells were stored in PBS at 4°C. For paraformaldehyde fixation, cells were washed in PBS, fixed in 4% paraformaldehyde for 10 min at room temperature, and stored at 4°C thereafter. For immunofluorescence of paraformaldehyde fixed cells, cells were permeabilised in 0.1% Triton X-100 in PBS for 1-5 minutes, washed in PBS, and blocked in blocking buffer [4% goat serum, 1% BSA in PBS-Tween (0.05%)] for at least 30 minutes at room temperature. After washing in PBS, cells were incubated with the appropriate antibodies diluted in blocking buffer for 30 minutes at room temperature, washed, and then incubated with the appropriate secondary Alexa-Fluor-488-conjugated anti-rabbit IgG, Alexa-Fluor-546-conjugated anti-mouse IgG or Alexa-Fluor-647-conjugated anti-mouse IgG antibodies (Molecular Probes). Samples were examined under a Zeiss LSM510 confocal immunofluorescence microscope. The antibody dilutions were as follows: NuMA polyclonal (1:300), NuMA monoclonal (1:100), lamin A/C (1:100), UL17 (1:200), ICP8 (1:100), FLAG monoclonal (1:100).

Time lapse confocal imaging of live cells

For live cell imaging, cells were cultured in a CO_2-system chamber using the PECON Heating insert P that was mounted directly onto the stage of the Zeiss Axiovert 200M microscope. The chamber was maintained at 37°C, 5% CO_2 in a humid atmosphere with Tempcontrol 37-2 and CTI-Controller 3700. Vero cells were seeded onto culture dishes with a glass bottom (Mat Tek Corp.) and transfected with pcmRFP-NuMA the next day. 20-24 hours later, cells were infected with F-VP26/GFP at a MOI of 5 PFU/cell. The infected cells were propagated in Phenol-Red-free D-MEM supplemented with 1% calf serum, 100 units/ml penicillin, 100 g/ml streptomycin, and 2 mM glutamine. Cells were examined at high magnification using a 63× lens with oil from 4 hours to 20-24 hours post infection. 20 to 25 *z*-axis confocal 0.37-0.5 μm sections (depending on the sample) were obtained at 488 nm and 543 nm excitations every 10 minutes with a Zeiss LSM510. All time-lapse pictures for a certain time point were projected using the LSM software onto a single plane to give all the fluorescence information of the infected cell. The projected pictures (six per hour) were sequenced to generate the movie (Movie 1).

Transfection of siRNAs

Stealth siRNAs (20 μM siNuMA and siCont) were obtained from Invitrogen. The siRNA sequence targeting NuMA was from position 3501-3525 relative to the start codon. HEp-2 cells were seeded at a 1:10 dilution (1×10^5 cells per dish) onto 35-mm culture dishes and transfected with 4 μl siRNA and 5 μl lipofectamine 2000 (Invitrogen) in 500 μl OPTI-MEM (GIBCO) the next day. The medium was replaced with growth medium (without antibiotics) 5 hours after transfection. The cells were analysed 3 days post transfection. Cell viability was monitored by Trypan-Blue exclusion. For normalisation of viral yield per cell, infected cells were trypsinised and counted. Each result of viral PFU was normalised to 10^6 cells.

Chemicals

Phosphonoacetic acid, cytochalasin D and nocodazole (Sigma), latrunculin A and 3-aminobenzamide (Calbiochem), Z-VAD-FMK (Biomol) were all solubilised in DMSO (Wako) and filter sterilised before use.

We are grateful to Duane Compton for providing wild-type NuMA, mutant cDNAs and the NuMA polyclonal antibody. We also thank Andreas Merdes for the GFP-NuMA plasmid and discussions, Aleksandra Snyder and David Johnson (Oregon Health & Sciences University, Portland, OR) for the F-VP26/GFP virus. Finally, we thank Kazuko Nagamoto and Eiko Iwata for their technical assistance. This work was supported by Grants-in-aid for Scientific Research on Priority Areas from the Ministry of Education, Culture, Sport, Science and Technology of Japan (18073007 and 16017240).

References

Advani, S. J., Hagglund, R., Weichselbaum, R. R. and Roizman, B. (2001). Posttranslational processing of infected cell proteins 0 and 4 of herpes simplex virus 1 is sequential and reflects the subcellular compartment in which the proteins localise. *J. Virol.* **75**, 7904-7912.

Bjerke, S. L. and Roller, R. J. (2006). Roles for herpes simplex virus type 1 UL34 and US3 proteins in disrupting the nuclear lamina during herpes simplex virus type 1 egress. *Virology* **347**, 261-276.

Burkham, J., Coen, D. M. and Weller, S. K. (1998). ND10 protein PML is recruited to herpes simplex virus type 1 prereplicative sites and replication compartments in the presence of viral DNA polymerase. *J. Virol.* **72**, 10100-10107.

Chang, W., Dynek, J. N. and Smith, S. (2005). NuMA is a major acceptor of poly(ADP-ribosyl)ation by tankyrase 1 in mitosis. *Biochem. J.* **391**, 177-184.

Cleveland, D. W. (1995). NuMA: a protein involved in nuclear structure, spindle assembly, and nuclear re-formation. *Trends Cell Biol.* **5**, 60-64.
Compton, D. A. (2005). Regulation of mitosis by poly(ADP-ribosyl)ation. *Biochem. J.* **391**, e5-e6.
Compton, D. A. and Cleveland, D. W. (1994). NuMA, a nuclear protein involved in mitosis and nuclear reformation. *Curr. Opin. Cell Biol.* **6**, 343-346.
Compton, D. A. and Luo, C. (1995). Mutation of the predicted p34cdc2 phosphorylation sites in NuMA impair the assembly of the mitotic spindle and block mitosis. *J. Cell Sci.* **108**, 621-633.
Compton, D. A., Szilak, I. and Cleveland, D. W. (1992). Primary structure of NuMA, an intranuclear protein that defines a novel pathway for segregation of proteins at mitosis. *J. Cell Biol.* **116**, 1395-1408.
Everett, R. D. and Zafiropoulos, A. (2004). Visualisation by live-cell microscopy of disruption of ND10 during herpes simplex virus type 1 infection. *J. Virol.* **78**, 11411-11415.
Everett, R. D. and Murray, J. (2005). ND10 components relocate to sites associated with herpes simplex virus type 1 nucleoprotein complexes during virus infection. *J. Virol.* **79**, 5078-5089.
Farina, A., Feederle, R., Raffa, S., Gonnella, R., Santarelli, R., Frati, L., Angeloni, A., Torrisi, M. R., Faggioni, A. and Delecluse, H. J. (2005). BFRF1 of Epstein-Barr virus is essential for efficient primary viral envelopment and egress. *J. Virol.* **79**, 3703-3712.
Feierbach, B., Piccinotti, S., Bisher, M., Denk, W. and Enquist, L. W. (2006). Alpha-herpesvirus infection induces the formation of nuclear actin filaments. *PLoS Pathog.* **2**, e85.
Forest, T., Barnard, S. and Baines, J. D. (2005). Active intranuclear movement of herpesvirus capsids. *Nat. Cell Biol.* **7**, 429-431.
Fuchs, W., Klupp, B. G., Granzow, H., Osterrieder, N. and Mettenleiter, T. C. (2002). The interacting UL31 and UL34 gene products of pseudorabies virus are involved in egress from the host-cell nucleus and represent components of primary enveloped but not mature virions. *J. Virol.* **76**, 364-378.
Gonnella, R., Farina, A., Santarelli, R., Raffa, S., Feederle, R., Bei, R., Granato, M., Modesti, A., Frati, L., Delecluse, H. J. et al. (2005). Characterisation and intracellular localisation of the Epstein-Barr virus protein BFLF2: interactions with BFRF1 and with the nuclear lamina. *J. Virol.* **79**, 3713-3727.
Goshima, F., Watanabe, D., Takakuwa, H., Wada, K., Daikoku, T., Yamada, M. and Nishiyama, Y. (2000). Herpes simplex virus UL17 protein is associated with B capsids and colocalises with ICP35 and VP5 in infected cells. *Arch. Virol.* **145**, 417-426.
Gueth-Hallonet, C., Wang, J., Harborth, J., Weber, K. and Osborn, M. (1998). Induction of a regular nuclear lattice by overexpression of NuMA. *Exp. Cell. Res.* **243**, 434-452.
Harborth, J., Elbashir, S. M., Bechert, K., Tuschl, T. and Weber, K. (2001). Identification of essential genes in cultured mammalian cells using small interfering RNAs. *J. Cell Sci.* **114**, 4557-4565.
Hsu, H. L. and Yeh, N. H. (1996). Dynamic changes of NuMA during the cell cycle and possible appearance of a truncated form of NuMA during apoptosis. *J. Cell Sci.* **109**, 277-288.
Kallajoki, M., Weber, K. and Osborn, M. (1991). A 210 kDa nuclear matrix protein is a functional part of the mitotic spindle; a microinjection study using SPN monoclonal antibodies. *EMBO J.* **10**, 3351-3362.
Klupp, B. G., Granzow, H., Fuchs, W., Keil, G. M., Finke, S. and Mettenleiter, T. C. (2007). Vesicle formation from the nuclear membrane is induced by coexpression of two conserved herpesvirus proteins. *Proc. Natl. Acad. Sci. USA* **104**, 7241-7246.
Leach, N., Bjerke, S. L., Christensen, D. K., Bouchard, J. M., Mou, F., Park, R., Baines, J., Haraguchi, T. and Roller, R. J. (2007). Emerin is hyperphosphorylated and redistributed in herpes simplex virus type 1-infected cells in a manner dependent on both UL34 and US3. *J. Virol.* **81**, 10792-10803.
Lydersen, B. K. and Pettijohn, D. E. (1980). Human-specific nuclear protein that associates with the polar region of the mitotic apparatus: distribution in a human/hamster hybrid cell. *Cell* **22**, 489-499.
Maekawa, T., Leslie, R. and Kuriyama, R. (1991). Identification of a minus end-specific microtubule-associated protein located at the mitotic poles in cultured mammalian cells. *Eur. J. Cell Biol.* **54**, 255-267.
Merdes, A. and Cleveland, D. W. (1998). The role of NuMA in the interphase nucleus. *J. Cell Sci.* **111**, 71-79.
Merdes, A., Ramyar, K., Vechio, J. D. and Cleveland, D. W. (1996). A complex of NuMA and cytoplasmic dynein is essential for mitotic spindle assembly. *Cell* **87**, 447-458.
Merdes, A., Heald, R., Samejima, K., Earnshaw, W. C. and Cleveland, D. W. (2000). Formation of spindle poles by dynein/dynactin-dependent transport of NuMA. *J. Cell Biol.* **149**, 851-862.
Mettenleiter, T. C. (2004). Budding events in herpesvirus morphogenesis. *Virus Res.* **106**, 167-180.
Morris, J. B., Hofemeister, H. and O'Hare, P. (2007). Herpes simplex virus infection induces phosphorylation and delocalisation of emerin, a key inner nuclear membrane protein. *J. Virol.* **81**, 4429-4437.
Mou, F., Forest, T. and Baines, J. D. (2007). US3 of herpes simplex virus type 1 encodes a promiscuous protein kinase that phosphorylates and alters localisation of lamin A/C in infected cells. *J. Virol.* **81**, 6459-6470.
Muranyi, W., Haas, J., Wagner, M., Krohne, G. and Koszinowski, U. H. (2002). Cytomegalovirus recruitment of cellular kinases to dissolve the nuclear lamina. *Science* **297**, 854-857.
Nguyen, M. L. and Blaho, J. A. (2007). Apoptosis during herpes simplex virus infection. *Adv. Virus Res.* **69**, 67-97.
Park, R. and Baines, J. D. (2006). Herpes simplex virus type 1 infection induces activation and recruitment of protein kinase C to the nuclear membrane and increased phosphorylation of lamin B. *J. Virol.* **80**, 494-504.
Pederson, T. and Aebi, U. (2002). Actin in the nucleus: what form and what for? *J. Struct. Biol.* **140**, 3-9.
Price, C. M. and Pettijohn, D. E. (1986). Redistribution of the nuclear mitotic apparatus protein (NuMA) during mitosis and nuclear assembly. Properties of purified NuMA protein. *Exp. Cell Res.* **166**, 295-311.
Reynolds, A. E., Ryckman, B. J., Baines, J. D., Zhou, Y., Liang, L. and Roller, R. J. (2001). U(L)31 and U(L)34 proteins of herpes simplex virus type 1 form a complex that accumulates at the nuclear rim and is required for envelopment of nucleocapsids. *J. Virol.* **75**, 8803-8817.
Reynolds, A. E., Wills, E. G., Roller, R. J., Ryckman, B. J. and Baines, J. D. (2002). Ultrastructural localisation of the herpes simplex virus type 1 UL31, UL34, and US3 proteins suggests specific roles in primary envelopment and egress of nucleocapsids. *J. Virol.* **76**, 8939-8952.
Reynolds, A. E., Liang, L. and Baines, J. D. (2004). Conformational changes in the nuclear lamina induced by herpes simplex virus type 1 require genes U(L)31 and U(L)34. *J. Virol.* **78**, 5564-5575.
Scott, E. S. and O'Hare, P. (2001). Fate of the inner nuclear membrane protein lamin B receptor and nuclear lamins in herpes simplex virus type 1 infection. *J. Virol.* **75**, 8818-8830.
Simpson-Holley, M., Baines, J., Roller, R. and Knipe, D. M. (2004). Herpes simplex virus 1 U(L)31 and U(L)34 gene products promote the late maturation of viral replication compartments to the nuclear periphery. *J. Virol.* **78**, 5591-5600.
Simpson-Holley, M., Colgrove, R. C., Nalepa, G., Harper, J. W. and Knipe, D. M. (2005). Identification and functional evaluation of cellular and viral factors involved in the alteration of nuclear architecture during herpes simplex virus 1 infection. *J. Virol.* **79**, 12840-12851.
Snyder, A., Wisner, T. W. and Johnson, D. C. (2006). Herpes simplex virus capsids are transported in neuronal axons without an envelope containing the viral glycoproteins. *J. Virol.* **80**, 11165-11177.
Sun, Q. Y. and Schatten, H. (2006). Role of NuMA in vertebrate cells: review of an intriguing multifunctional protein. *Front. Biosci.* **11**, 1137-1146.
Taimen, P., Berghall, H., Vainionpaa, R. and Kallajoki, M. (2004). NuMA and nuclear lamins are cleaved during viral infection-inhibition of caspase activity prevents cleavage and rescues HeLa cells from measles virus-induced but not from rhinovirus 1B-induced cell death. *Virology* **320**, 85-98.
Tousson, A., Zeng, C., Brinkley, B. R. and Valdivia, M. M. (1991). Centrophilin: a novel mitotic spindle protein involved in microtubule nucleation. *J. Cell Biol.* **112**, 427-440.
Yamauchi, Y., Shiba, C., Goshima, F., Nawa, A., Murata, T. and Nishiyama, Y. (2001). Herpes simplex virus type 2 UL34 protein requires UL31 protein for its relocation to the internal nuclear membrane in transfected cells. *J. Gen. Virol.* **82**, 1423-1428.
Yamauchi, Y., Kiriyama, K., Kubota, N., Kimura, H., Usukura, J. and Nishiyama, Y. (2008). The UL14 tegument protein of herpes simplex virus type 1 (HSV-1) is required for efficient nuclear transport of the alpha transinducing factor VP16 and viral capsids. *J. Virol.* **82**, 1094-1106.
Yang, C. H., Lambie, E. J. and Snyder, M. (1992). NuMA: an unusually long coiled-coil related protein in the mammalian nucleus. *J. Cell Biol.* **116**, 1303-1317.